

FR 9201253

LAL 91-63
November 1991

Laboratoire de l'Accélérateur Linéaire

PROSPECTS FOR SUPERSYMMETRY DISCOVERIES AT
A 500 GEV e^+e^- COLLIDER

J.-F. Grivaz

*Invited talk at the Workshop on Physics and Experiments with
Linear Colliders, Saariselkä, Finland, September 9-14, 1991*

U.E.R
de
l'Université Paris-Sud



Institut National
de Physique Nucléaire
et
de Physique des Particules

Bâtiment 200 - 91405 ORSAY Cedex

ORIS 000000

Prospects for Supersymmetry Discoveries at a 500 GeV e^+e^- Collider

J.-F. Grivaz

Laboratoire de l'Accélérateur Linéaire, IN2P3-CNRS
et Université de Paris-Sud, F-91405 Orsay Cedex, France

Abstract

The potential of a 500 GeV electron-positron collider for the discovery of supersymmetry is confirmed. If the MSSM is valid, at least one of its neutral Higgs bosons will be discovered. Moreover, the simultaneous observation of the three neutral Higgs bosons predicted by the model could decisively prove it. As shown by analyses incorporating realistic beam conditions and detector performances, charginos or scalar leptons can be discovered even close to the kinematic limit in spite of large standard model backgrounds, unless they are practically mass degenerate with the lightest neutralino.

1 Introduction

1.1 General features of supersymmetric theories

One of the most severe diseases of the minimal standard model—known under the name of *gauge hierarchy problem*—is that the Higgs boson mass receives quadratically divergent contributions in the renormalization process. The only known way to stabilize it near the scale of electroweak symmetry breaking, while preserving the elementary nature of the scalar Higgs field, is low energy supersymmetry[1]. This is obtained at the expense of the introduction of a whole bestiary of new *supersymmetric particles*. These are grouped in *supermultiplets* with their ordinary partners, from which they differ by half a unit of spin, in such a way that the number of fermionic and bosonic degrees of freedom are equal within each supermultiplet. The minimal supermultiplet content (for colourless fields) is shown in Table 1, assuming for clarity $SU(2)_L \times U(1)_Y$ already broken to $U(1)_{EM}$.

spin-0	spin-1/2	spin-1
$\bar{l}_L \bar{l}_R$	l	
H	$\tilde{\gamma}$ $\tilde{H} \tilde{Z}$	γ Z
$h A$	\tilde{h}	
H^\pm	$\tilde{H}^\pm \tilde{W}^\pm$	W^\pm

Table 1: Minimal supermultiplet content

To each of the left and right helicity states of a spin-1/2 lepton is associated a spin-0 partner; and the same holds for quarks. To the massless spin-1 photon, which has two helicity states, is associated a spin-1/2 Majorana fermion, also with two helicity states, the photino $\tilde{\gamma}$; and the same holds for the gluon and the gluino. The massive spin-1 Z boson has three helicity states, it is therefore not sufficient to associate it with a single spin-1/2 Majorana zino \tilde{Z} ; but the introduction of a Higgs boson H , with one bosonic degree of freedom, and of a second spin-1/2 Majorana fermion, the higgsino \tilde{H} , allows the gauge anomalies to be cancelled in this supermultiplet. The same holds for the W^\pm supermultiplet, which contains two spin-1/2 fermions, the wino \tilde{W}^\pm and the charged higgsino \tilde{H}^\pm , and a charged Higgs boson H^\pm . The occurrence of a charged Higgs boson indicates that at least two Higgs doublets are needed, which is anyway necessary in supersymmetric theories to give masses to both the up and down-type

quarks. With two Higgs doublets, two more neutral Higgs bosons survive once the weak vector bosons have acquired their masses, the CP -even h and the CP -odd A , which are associated with a spin-1/2 Majorana fermion, the higgsino \tilde{h} . Beyond this minimal structure, the most common extension is the introduction of an additional complex Higgs singlet and of its spin-1/2 partner, often called singlino.

Since, for instance, there is no scalar particle degenerate in mass with the electron, supersymmetry must be broken. Little is known on general grounds on the breaking mechanism except that, if the hierarchy problem is to remain solved, the mass splitting within the various supermultiplets cannot substantially exceed a TeV/c^2 or so. As supersymmetry is broken, not only is the mass degeneracy within the supermultiplets lifted, but also mixing occurs among the interaction eigenstates to form mass eigenstates. Model building suggests that the mixing among the scalar partners of the matter fermions is negligible, except possibly for the scalar tops. On the other hand, substantial $\tilde{W}^\pm - \tilde{H}^\pm$ mixing is expected, resulting in two mass eigenstates called “charginos”, the lighter of which is denoted χ^\pm . Similarly, the photino, the zino and the neutral higgsinos mix to form at least four mass eigenstates called “neutralinos” and denoted $\chi, \chi', \chi'', \dots$ following the increasing mass ordering.

The exchange of supersymmetric particles could induce an unacceptably short proton lifetime. A natural, although not unique, way to prevent this is to introduce a new conserved multiplicative quantum number, R-parity, defined for a given particle as $R = (-1)^{2S+3B+L}$. Here, S is the particle spin, B is its baryon number, and L its lepton number. It can be seen that the ordinary particles have $R = 1$ while their supersymmetric partners have $R = -1$. The conservation of R-parity, which will be systematically assumed in the following, has important experimental consequences:

- Supersymmetric particles are produced in pairs.
- An odd number of supersymmetric particles is emitted in every supersymmetric particle decay, and any decay cascade ends up with the LSP, the “lightest supersymmetric particle”.
- The LSP is stable.

Cosmological arguments strongly suggest that the LSP is neutral and colourless. The most popular LSP candidate is χ , the lightest of the neutralinos, and, although other less natural possibilities are viable, this assumption will consistently be made in the following.

The LSP interacts with ordinary matter *via* the exchange of heavy particles (Z boson, scalar quark or electron, as shown in Fig. 1); it is therefore neutrino-like, which is the origin of the celebrated signature of supersymmetric particle production, namely the *missing energy* carried away by the LSP resulting from the produced supersymmetric particle decay.

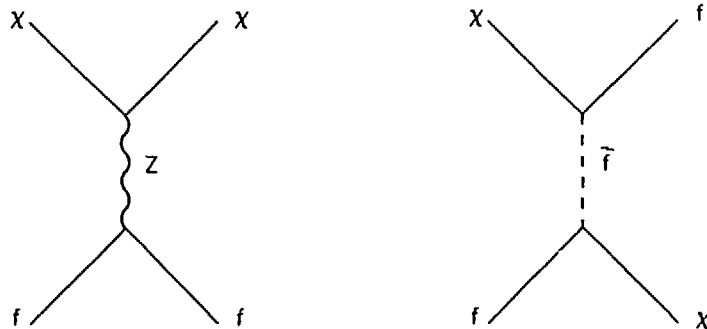


Figure 1: Diagrams involved in the interaction of the LSP with ordinary matter

1.2 Basics of the MSSM

The simplest and most widely discussed supersymmetric model is the MSSM, the “minimal supersymmetric extension of the standard model”[1]. It is derived from a Lagrangian exactly supersymmetric at some Grand Unification scale, except for a set of explicit “soft supersymmetry breaking terms”. The model is minimal in two respects:

- The field content is minimal. In particular, there are only two Higgs doublets, and therefore no more Higgs bosons than the ones appearing in Table 1, and therefore also exactly four neutralinos.
- The number of supersymmetry breaking parameters is minimal.

The number of unknown parameters, new with respect to the minimal standard model, is fairly small:

- μ , a supersymmetric mass term which mixes the two Higgs doublets,
- M , a gaugino mass term common to all the gauge boson supersymmetric partners,
- m_0 , a scalar mass term common to all the matter fermion supersymmetric partners, and also to the Higgs bosons,
- A , the coefficient of a trilinear coupling which will not be needed in the following,

where the three last quantities explicitly break supersymmetry. This small number of parameters is at the origin of the predictivity of the MSSM.

The low energy theory is derived from this Lagrangian using the renormalization group equations. On the way, the neutral components of the two Higgs doublets develop vacuum expectation values v_1 and v_2 such that the up-type quark masses are proportional to v_2 while the down-type quark and the charged lepton masses are proportional to v_1 . The ratio v_2/v_1 will be denoted $\tan\beta$ in the following. In order that the electroweak symmetry be properly broken and that no disaster occur such as, for instance, spontaneous lepton number violation, the unknown parameters are in fact constrained to lie in a rather limited range. In particular, $\tan\beta$ has to be larger than unity and should not exceed m_t/m_b .

In the same way as the unified gauge coupling constants get renormalized differently at low energy, the universal gaugino mass term M gets renormalized into M_1 , M_2 and M_3 , where the labels refer to the appropriate gauge groups. Unification is preserved in the form of mass relations such as

$$M_1 = \frac{5}{3} \tan^2 \theta_W M_2 \quad \text{and} \quad M_3 = \frac{\alpha_S}{\alpha_{EM}} \sin^2 \theta_W M_2.$$

From these relations, it can be inferred that the gluino should be at least 5.5 times heavier than the lightest neutralino and 3.5 times heavier than the lighter chargino.

Similarly, the supersymmetric partners of the quarks and of the leptons on the one hand, of the left and of the right-handed helicity states of those quarks and leptons on the other get renormalized differently. The scalar quarks are expected to be substantially heavier than the scalar leptons, and the partners of the left handed helicity states heavier than those of the right handed helicity states.

1.3 Outline

In the following, the two characteristic manifestations of supersymmetry will be addressed, namely

- a Higgs boson structure richer than the one of the minimal standard model but also, at least in the MSSM, highly constrained,
- the production of supersymmetric particles,

and the discovery potential of a 500 GeV e^+e^- collider will be assessed accordingly.

2 Testing the Higgs sector of the MSSM

2.1 Introduction

In general two-Higgs-doublet models, six parameters are necessary to describe the Higgs boson physical spectrum:

- four masses, namely m_h and m_H for the two CP -even neutral bosons, m_A for the CP -odd neutral boson, and m_{H^\pm} for the charged boson pair,
- the mixing angle α in the CP -even sector, and
- $\tan\beta$, the ratio of the two vacuum expectation values.

When supersymmetry is imposed, strong constraints result among these parameters[1], of which two only remain independent. These can conveniently be chosen as m_A and $\tan\beta$, or alternatively as m_A and m_h . In addition, mass relations arise which make a search in e^+e^- collisions at energies not exceeding a few hundred GeV very promising. For instance, it can be inferred from the tree-level Higgs potential that $m_h < m_Z < m_H$ and $m_h < m_A$, making LEP-200 an ideal machine to discover at least the lighter of the CP -even Higgs bosons.

It has however been realized recently that substantial radiative corrections deeply modify these relations when the large top-quark mass m_t is taken into account[1]. In the MSSM, the tree-level squared mass matrix in the CP -even sector is modified at the one-loop level by terms of order

$$\varepsilon = \frac{\varepsilon_0}{\sin^2\beta} \quad \text{with} \quad \varepsilon_0 = \frac{3g^2 m_t^4}{8\pi^2 m_W^2} \log\left(1 + \frac{m_0^2}{m_t^2}\right),$$

a quantity which takes the value $(60 \text{ GeV}/c^2)^2$ if $m_t = 140 \text{ GeV}/c^2$ and $m_0 = 1 \text{ TeV}/c^2$ (this set of top and universal scalar mass values will be called “typical” in the following). Indeed, the precise expression of ε also depends on A and μ , but the influence of these parameters on the values of m_h and m_H is much smaller; they have thus been set to zero in the following numerical calculations. The most important relation for experimental searches, namely $m_h < m_Z$, now becomes

$$m_h < \sqrt{m_Z^2 + \varepsilon_0},$$

from which it results that $m_h < 110 \text{ GeV}/c^2$ for the typical set of parameters. Such an upper limit is too high for LEP-200 to be guaranteed to discover a Higgs boson, but it is well within the reach of a 500 GeV e^+e^- collider. This remains true for more extreme choices of parameters, the upper bound becoming $180 \text{ GeV}/c^2$ if $m_t = 200 \text{ GeV}/c^2$ and $m_0 = 5 \text{ TeV}/c^2$.

The main neutral Higgs boson production mechanisms in e^+e^- collisions are

- the bremsstrahlung process $e^+e^- \rightarrow h/H Z$,
- the WW fusion process $e^+e^- \rightarrow h/H \nu\bar{\nu}$, and
- the associate production $e^+e^- \rightarrow h/H A$.

The bremsstrahlung and WW fusion process cross-sections are equal to the corresponding ones for the minimal standard model Higgs boson, up to reduction factors of $\sin^2(\beta - \alpha)$ for h and of $\cos^2(\beta - \alpha)$ for H . Conversely, the associate production cross-sections are proportional to $\cos^2(\beta - \alpha)$ for hA and to $\sin^2(\beta - \alpha)$ for HA . The dependence of $\sin^2(\beta - \alpha)$ on $m_{h/H}$ and on m_A is shown in Fig. 2 for the typical set of parameters.

2.2 Neutral Higgs boson searches at 500 GeV

The following discussion of the potential of a 500 GeV e^+e^- collider to probe the Higgs sector of the MSSM closely follows P. Janot's presentation in parallel session and Ref. [2].

Searches for the neutral Higgs bosons of the MSSM have already been performed at LEP in decays of on-shell Z bosons. The complementary processes $Z \rightarrow hZ^*$ and $Z \rightarrow hA$ have been investigated, and excluded domains in the parameter space of the MSSM have been inferred[5], as shown in Fig. 3 (the excluded (m_H, m_A) couples are simply a reflection of the corresponding (m_h, m_A) ones). Similar searches will be pursued at LEP-200. Assuming that 500 pb⁻¹ are accumulated, and that the search efficiencies are not worse than the ones presently achieved, the domain which can be explored before a high energy e^+e^- linear collider begins to operate should be enlarged as shown in Fig. 3.

In the domain which cannot be explored at LEP-200, the dominant neutral Higgs boson production mechanisms at a 500 GeV e^+e^- collider depend on the exact location in the $(m_A$ vs $m_{h/H})$ plane (see Fig. 3):

- In region (1), $e^+e^- \rightarrow hZ$ and $e^+e^- \rightarrow h\nu\bar{\nu}$ occur with large rates since $\sin^2(\beta - \alpha)$ is close to unity, while $e^+e^- \rightarrow hA$ or HZ are suppressed accordingly, and $e^+e^- \rightarrow HA$ is kinematically forbidden.
- In region (2), the situation is the same as in region (1), except that $e^+e^- \rightarrow HA$ is now open and large too, except for some phase space suppression near the kinematic limit.
- In region (3), the situation is reversed since $\cos^2(\beta - \alpha)$ is close to unity. $e^+e^- \rightarrow HZ$ and $e^+e^- \rightarrow H\nu\bar{\nu}$ occur with large rates, and so does $e^+e^- \rightarrow hA$, while $e^+e^- \rightarrow hZ$, $e^+e^- \rightarrow h\nu\bar{\nu}$ and $e^+e^- \rightarrow HA$ are suppressed.

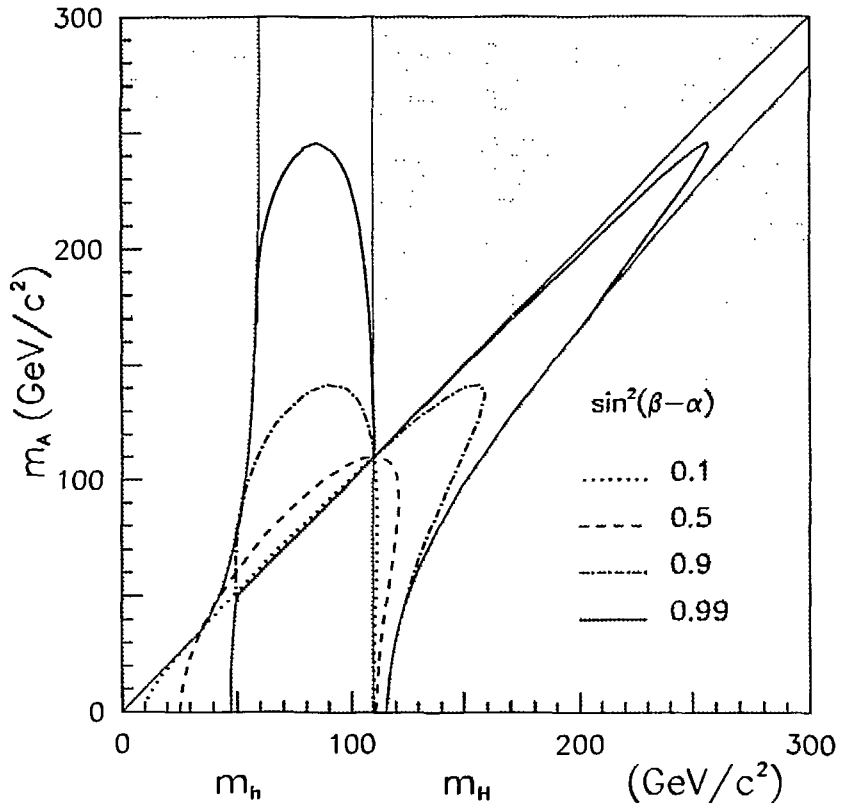


Figure 2: In the (m_A vs $m_{h/H}$) plane, equal value contours for $\sin^2(\beta - \alpha)$. The horizontal axis refers to m_h for values smaller than 110 GeV/c² and to m_H for higher values. The grey area is forbidden for the typical set of parameters.

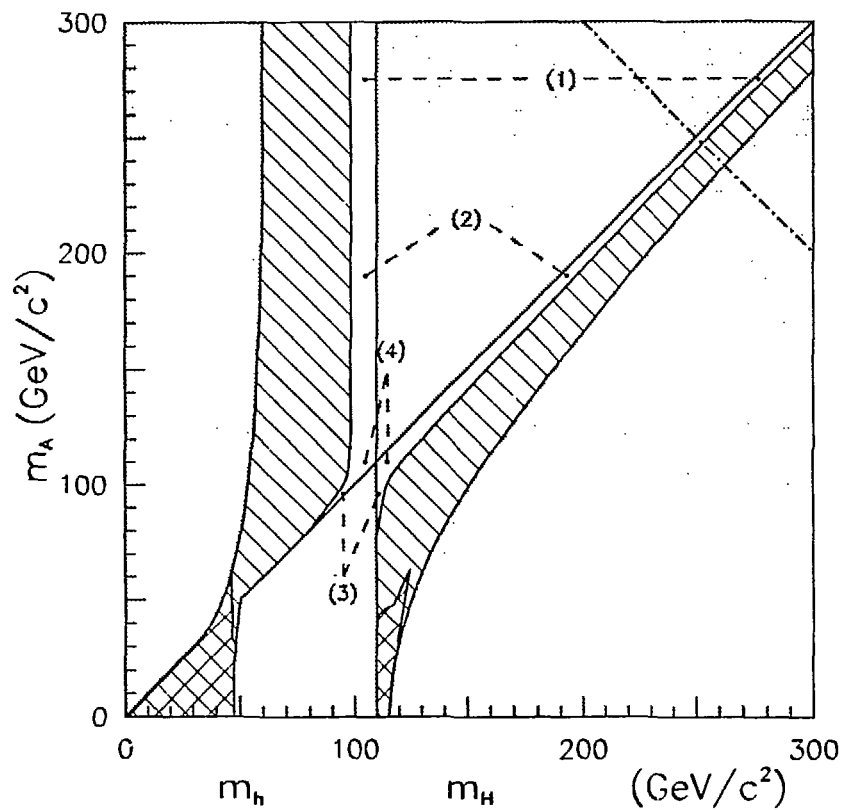


Figure 3: In the $(m_A$ vs $m_{h/H})$ plane, and for the typical set of parameters: the domain presently excluded, shown cross-hatched, and the domain which can be explored at LEP-200, shown hatched. The dash-dotted line is the kinematic limit for HA associate production at 500 GeV. See also the caption of the previous figure, and the text for the characteristics of regions (1) to (4).

- In region (4), all processes are kinematically allowed. None occurs at the maximal rate, but none is strongly suppressed either, and the three neutral Higgs bosons have similar masses.

The cross-section for the sum of the bremsstrahlung processes is slightly larger than 60 fb and almost constant in all of the domain to be explored. Therefore, a standard model-like Higgs boson must be discovered using the well known methods reported in Refs. [3] and [4], or the MSSM is ruled out. This Higgs boson is h in regions (1) and (2), H in region (3) and, given the mass resolutions that can be expected, a practically mass-degenerate superposition of h and H in region (4). In addition, if the top-quark mass is $140 \text{ GeV}/c^2$, the mass of this Higgs boson must lie between ~ 100 and $\sim 140 \text{ GeV}/c^2$ (assuming m_0 does not exceed $\sim 5 \text{ TeV}/c^2$), or the MSSM is also ruled out. The upper bound of the mass domain in which such a Higgs boson has to be found increases to no more than $\sim 200 \text{ GeV}/c^2$ if $m_t = 200 \text{ GeV}/c^2$ (with the same assumption for m_0 as above), which remains well within the reach of a $500 \text{ GeV } e^+e^-$ collider.

Let it now be assumed that such a standard model-like Higgs boson is discovered. The question arises of how this situation can be disentangled from the production of a real standard model Higgs boson. This can be achieved by the observation of one of the associate production reactions. However, if $m_A \gtrsim 200 \text{ GeV}/c^2$, HA production is phase-space suppressed, or even forbidden, while hA production is suppressed due to the small value of $\cos^2(\beta - \alpha)$; the question will therefore remain unsettled in this unfortunate situation. On the other hand, if $m_A \lesssim 200 \text{ GeV}/c^2$, the cross-section for the sum of the associate production processes is larger than 10 fb:

- Either HA production dominates, with $m_H \sim m_A$; this is the case in region (2).
- Or hA production dominates, with $m_h \sim m_A$; this is the case in region (3).
- Or both hA and HA contribute, with $m_h \sim m_A \sim m_H$; this is the case in region (4).

An analysis has been developed, described in detail in Ref. [2], which takes advantage of the fact that the probability for any of h , H or A to decay into a $\tau^+\tau^-$ pair is of the order of 8% in all of the relevant domain. A final state consisting of a $\tau^+\tau^-$ pair accompanied by a hadronic system therefore arises in $\sim 15\%$ of the cases. A measurement of the directions of the taus and of the velocity of the hadronic system provides enough constraints, together with the knowledge of the center-of-mass energy, for both the $\tau^+\tau^-$ and hadronic system masses to be reconstructed with a resolution of $\sim 3 \text{ GeV}/c^2$, even allowing for an additional photon, from initial state radiation or from beamstrahlung, emitted along the beam direction and therefore undetected. In addition, the same

method can be applied to the bremsstrahlung processes, but with a somewhat reduced efficiency since the $Z \rightarrow \tau^+\tau^-$ decay branching ratio is only 3.5%.

The distribution of the thus reconstructed invariant masses is expected to show three peaks: one at m_Z , one at m_A , and one at m_h or m_H , while the other peak (at m_H or m_h) is practically indistinguishable from the one at m_A . Examples of such distributions are shown in Fig. 4. They have been obtained assuming an integrated luminosity of 10 fb^{-1} , using a realistic detector simulation (see Section 3.2.3), and taking into account all the standard model backgrounds (see Section 3.2.2).

The various characteristic situations are (see Fig. 4):

- (A) No Higgs boson produced. Only the Z peak is visible, arising from the irreducible background from $e^+e^- \rightarrow ZZ$.
- (B) HZ and hA produced, as in region (3). Peaks show at the Z , H and “ h and A ” masses. Even if the Z peak coalesces with the “ h and A ” one as in (C), the H peak remains visible, and the signal to background ratio in the Z peak is comfortable.
- (D) hZ , HZ , hA and HA all produced, as in region (4). The exact number of distinct peaks depends on the location in region (4), but the situation can never be mistaken with the production of a single Higgs boson.
- (E) hZ and HA produced, as in region (2). Peaks show at the Z , h and “ H and A ” masses.
- (F) Only hZ is produced. This is the unfortunate situation in region (1), but this demonstrates that the method can also be successfully applied to a standard model Higgs boson.

The goal of discriminating the MSSM from the minimal standard model, a clarification which may remain necessary even if a standard model-like Higgs boson has previously been discovered at LEP-200, is thus shown to be achievable with an integrated luminosity of a few fb^{-1} , at least as long as m_A and $m_H \lesssim 200 \text{ GeV}/c^2$. This conclusion is not affected if the top quark mass is increased to $200 \text{ GeV}/c^2$, or the scalar mass to a few TeV/c^2 .

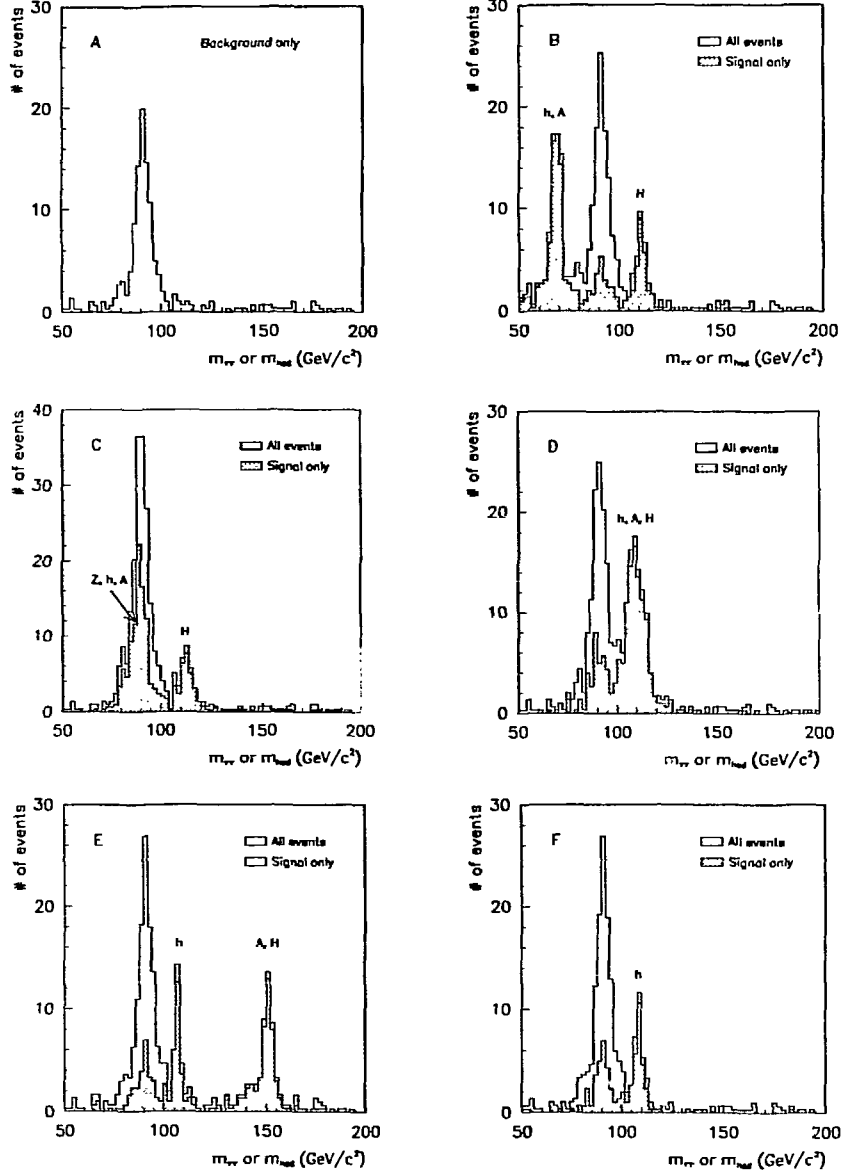


Figure 4: Distributions of the $\tau^+\tau^-$ and hadronic masses with no signal (A); for $m_A = 70 \text{ GeV}/c^2$ (B), m_Z (C), $110 \text{ GeV}/c^2$ (D), $150 \text{ GeV}/c^2$ (E) and $500 \text{ GeV}/c^2$ (F) (with $\tan\beta = 10$ (except in (D) where $\tan\beta = 30$), $m_t = 140 \text{ GeV}/c^2$ and $m_{\tilde{t}_1} = 1 \text{ TeV}/c^2$).

3 Searching for supersymmetric particles

3.1 Introduction

While hadron colliders operating at the highest energies are known to be the most appropriate tool to search for the strongly interacting supersymmetric particles, namely scalar quarks and gluinos, e^+e^- colliders have demonstrated, at LEP in particular, their ability to extend up to their kinematic limit the discovery reach for the weakly interacting supersymmetric particles, namely scalar leptons and gauginos. Today's limits on scalar quark and gluino masses, as provided by CDF at the Tevatron[6], exceed $100 \text{ GeV}/c^2$, while the limits on scalar lepton and chargino masses, as obtained at LEP[7], are essentially given by half the Z mass. Tomorrow's limits should extend to $\sim 300 \text{ GeV}/c^2$ for gluinos at the Tevatron, and to $\sim 80 \text{ GeV}/c^2$ for charginos at LEP-200[8].

In most supersymmetric grand unification schemes, it turns out that the results obtained at hadron and at e^+e^- colliders are and will remain similarly constraining since, in such schemes, it is commonly expected that the gluino mass should be approximately 3.5 times larger than the mass of the lighter chargino, at least. In this respect, the discovery reach of the LHC and of the SSC on the one hand, extending to gluino masses of a TeV/c^2 or so[9], and that of a $500 \text{ GeV } e^+e^-$ collider on the other hand, extending to gaugino masses close to $250 \text{ GeV}/c^2$, appear quite similar. However, there is little doubt that further detailed studies of the produced supersymmetric particles can be performed more accurately at an e^+e^- collider.

In this section, the arguments demonstrating that the discovery potential of a $500 \text{ GeV } e^+e^-$ collider is indeed at the level expected are summarized. Investigations of the capabilities of a high energy e^+e^- linear collider for supersymmetric particle searches have previously been performed[10]; the novel aspects that have been emphasized for the present studies are:

- a comprehensive account of the standard model background processes,
- an assessment of the impact of possibly severe beamstrahlung conditions, and
- a realistic detector simulation.

3.2 Common features

3.2.1 Analysis strategy

As already stated, the distinctive signature for the production of supersymmetric particles is, with R-parity conserved, the missing energy-momentum carried away by the LSPs. Since, at a $500 \text{ GeV } e^+e^-$ collider with $\mathcal{L} = 10^{33} \text{ cm}^{-2} \text{ s}^{-1}$, the pair production of LSPs in a “neutrino counting” type experiment (i.e.

through $e^+e^- \rightarrow \chi\chi\gamma$) has too small a rate to be observable, the most natural line of attack is to search for the pair production of NLSPs (here, the NLSP is “the next to lightest supersymmetric particle”). For instance, the NLSP could be a scalar electron which decays to an electron and to the lightest neutralino. The process to be searched for would then be $e^+e^- \rightarrow \tilde{e}_R^+\tilde{e}_R^-$ followed by $\tilde{e}_R \rightarrow e\chi$, leading to the signature of an acoplanar e^+e^- pair.

It may happen however that the NLSP is invisible too. The typical example is that of a scalar neutrino $\tilde{\nu}$ decaying according to $\tilde{\nu} \rightarrow \nu\chi$. The search should then be redirected toward the NNLSP (in an obvious notation), with the NLSP playing the role normally held by the LSP. In the above example, the NNLSP could be a chargino which decays into a lepton and a scalar neutrino. Here again, the signature of the pair production of supersymmetric particles would be an acoplanar pair of leptons.

Associate production of the LSP with a heavier supersymmetric particle has not been considered here. Such a process, like for instance $e^+e^- \rightarrow \chi\chi'$, could well be the one with the lowest threshold among those leading to non-invisible final states. It turns out, however, that the corresponding cross-section is always uninterestingly small, at least in the MSSM, when all the pair production reactions are kinematically forbidden.

To summarize, it is sufficient to consider the reactions

- $e^+e^- \rightarrow \chi^+\chi^-$, with $\chi^\pm \rightarrow \chi W^{(*)}$ or $\chi^\pm \rightarrow l\bar{\nu}$, and
- $e^+e^- \rightarrow \tilde{l}^+\tilde{l}^-$, with $\tilde{l} \rightarrow l\chi$

in order to assess the ability of a 500 GeV e^+e^- collider to discover supersymmetric particles.

3.2.2 Background processes

The cross-sections for the relevant signal processes range typically from the few tens of femtobarn level to the fraction of a picobarn. Therefore, all standard model processes with cross-sections in excess of ~ 100 fb are to be carefully considered.

In past and present experiments at e^+e^- colliders, a most common source of final states with apparent missing energy-momentum is the radiative annihilation $e^+e^- \rightarrow f\bar{f}\gamma$ because the radiated photon tends to be emitted close to the e^+e^- axis and therefore to escape undetected in the beam pipe. This background is even more severe at 500 GeV because of the large probability for a photon to be radiated with an energy such that the remaining effective centre-of-mass energy is close to the Z resonance peak. The cross-section for $e^+e^- \rightarrow \gamma^*$ or Z^* , with such initial state radiation included, is as large as 17 pb at 500 GeV. In addition, real beamstrahlung may occur, making the situation even worse.

Fortunately, this kind of background is easily fought by requiring that the missing momentum be directed away from the beam direction or, equivalently, that missing *transverse* momentum p_t be present rather than simply missing momentum. For the same reason, the acoplanarity variable is to be preferred to the acollinearity, the transverse visible or missing masses to the visible or missing masses, and so on...

A novel issue, compared to searches for supersymmetry performed at lower energies, comes from the production of W pairs. Not only this process has a large cross-section of 7 pb at 500 GeV, but in addition this reaction can produce final states with true missing energy-momentum when at least one of the W 's decays through $W \rightarrow l\nu$. Because of these two features, this background process deserves the utmost attention when cuts are chosen to increase the signal to background ratio.

Besides $f\bar{f}$ and W^+W^- , the only two-body final state which may be a source of concern is ZZ . Its production cross-section of 0.6 pb is much smaller, but it creates a severe background when $Z \rightarrow \nu\bar{\nu}$, which happens in a third of the cases.

Three-body final states also are a substantial background source at these high energies:

- $e^+e^- \rightarrow W e \nu$ proceeds *via* γW fusion, with a large cross-section of 5 pb. The spectator electron tends to remain in the beam pipe while the neutrino takes a substantial transverse momentum because of the exchanged W propagator. The observable final state thus consists of a single W with large missing p_t .
- $e^+e^- \rightarrow Z e e$ results from virtual Compton scattering, also with a large cross-section of 6 pb. But, although one of the electrons tends to escape in the beam pipe, there is no reason for the visible eZ final state to show any substantial missing p_t .
- $e^+e^- \rightarrow Z \nu\bar{\nu}$ occurs *via* WW fusion, with a rather small cross-section of 0.2 pb. However, because of the exchanged W propagators, there is substantial missing p_t taken away by the $\nu\bar{\nu}$ system.

Some processes leading to four-body final states can also have large cross-sections. The rate is even enormous (tens of nanobarns !) for $e^+e^- \rightarrow e e f \bar{f}$ which takes place *via* virtual $\gamma\gamma$ scattering. In such a reaction, the electrons emerge at low angles with respect to the beam axis, but the $f\bar{f}$ system is bound not to exhibit more p_t than can be balanced by the undetected electrons; otherwise such spectator electrons must be detected. For $e^+e^- \rightarrow e e W W$, the cross-section of 0.2 pb is much more manageable, but this is a background source if one of the W 's decays leptonically. The other four-body final states, like $e\nu Z W$ or $\nu\bar{\nu} W W$ have production cross-sections lower than 10 fb and thus need not be considered further.

Depending on the values of their cross-sections, 1 to 10 fb^{-1} of all the above standard model processes have been generated for background study purposes, using the PYTHIA Monte Carlo program[11] (except for the $e^+e^- \rightarrow Z\nu\bar{\nu}$ reaction for which a specific generator, based on Ref. [12], has been used). A top-quark mass value of $140 \text{ GeV}/c^2$ has been taken. The beamstrahlung conditions chosen were the ones specified below.

3.2.3 Simulation conditions

In all signal and background simulations, highly conservative conditions have been implemented.

As far as the detector is concerned, the following have been assumed:

- The detector coverage extends down to polar angles of 18° and 10° with respect to the beam axis for charged particle track reconstruction and for calorimetric measurements, respectively.
- The detection thresholds for charged and neutral particles are $100 \text{ MeV}/c$ and 200 MeV , respectively.
- The charged particle momentum resolution is $\Delta p_t/p_t = 1.5 \cdot 10^{-3} p_t$, with p_t in GeV/c .
- The electromagnetic and hadronic calorimetry resolutions are $\Delta E/E = (0.17/\sqrt{E} + 0.03)$ and $0.80/\sqrt{E}$, respectively, with E in GeV .
- Electron and muon identifications are taken to be perfect for well isolated high energy charged particles.
- Finally, an energy flow algorithm is available, which can reconstruct the total energy with a resolution $\Delta E/E \simeq 0.70/\sqrt{E}$, with E in GeV .

Such performances are already available in today's LEP detectors.

As far as the beam is concerned, a rather extreme beamstrahlung spectrum has been assumed, of the "Palmer G" type. The corresponding effective e^+e^- luminosity is shown in Fig. 5. It has to be kept in mind that the effect is much worse when this effective luminosity is convoluted with an annihilation cross-section which has the characteristic $1/s$ dependence. The result thus obtained in the case of W pair production is also shown in Fig. 5. A quarter of the pairs produced have an effective mass below $400 \text{ GeV}/c^2$ instead of the nominal $500 \text{ GeV}/c^2$. In addition, with such a beamstrahlung spectrum, it is not unfrequent that more than one photon is emitted prior to the e^+e^- collision.

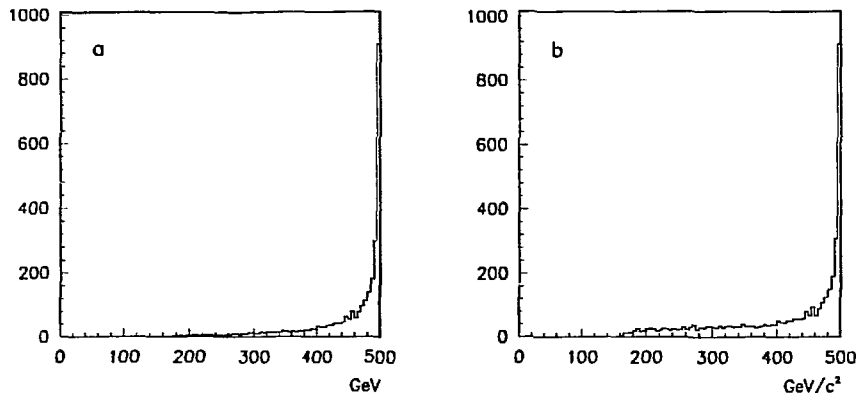


Figure 5: Effective e^+e^- luminosity (a), and mass spectrum of the produced W pairs (b).

3.3 Search for charginos

3.3.1 Chargino production and decay, signal topologies

The $\chi^+\chi^-$ pair-production mechanisms in e^+e^- collisions are virtual γ or Z exchange in the s -channel, and also $\tilde{\nu}$ exchange in the t -channel (see Fig. 6), the latter involving only the gaugino component in χ^\pm . For light enough scalar neutrinos, the interference between the s and t -channel exchange amplitudes can be large and destructive. The production cross-section depends on m_{χ^\pm} , the chargino mass, on the field content of χ^\pm and on $m_{\tilde{\nu}}$, the $\tilde{\nu}$ mass. For instance, when $m_{\chi^\pm} = 200 \text{ GeV}/c^2$, the value of the cross-section is as large as 500 fb if χ^\pm is a pure gaugino and $m_{\tilde{\nu}} = 1 \text{ TeV}/c^2$; it decreases to a minimum of 95 fb as $m_{\tilde{\nu}}$ is reduced to 250 GeV/c^2 before increasing again as $m_{\tilde{\nu}}$ is reduced further.

The chargino decay pattern depends on whether $m_{\tilde{\nu}}$ is larger or smaller than m_{χ^\pm} :

- If $m_{\tilde{\nu}} > m_{\chi^\pm}$, the final states are $\chi f \bar{f}'$, reached *via* real or virtual W exchange or *via* virtual scalar lepton or quark exchange (see Fig. 7). The latter contribution is however negligible if all scalar leptons and quarks are substantially heavier than the W or if the two-body decay $\chi^\pm \rightarrow \chi W$ is kinematically accessible. In such cases, 70% of the final states are hadronic while $\chi l \nu$ contributes 10% for each of the three lepton flavours.

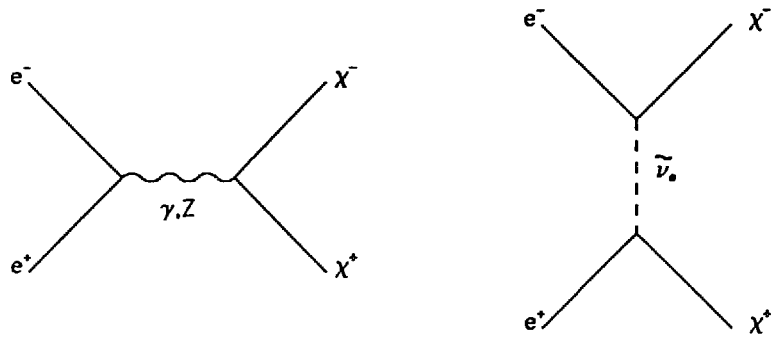


Figure 6: Diagrams involved in chargino production.

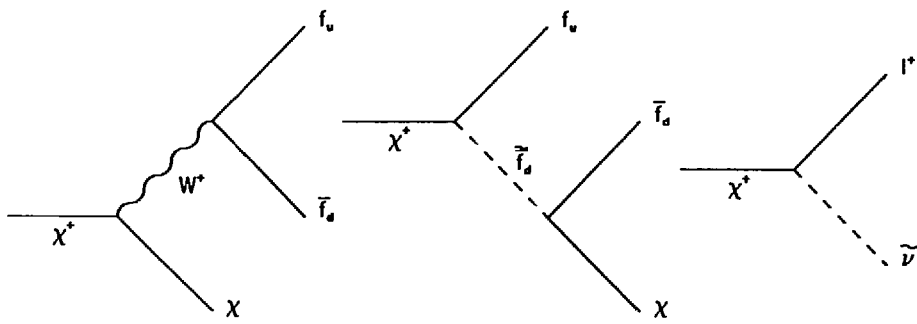


Figure 7: Diagrams involved in chargino decays.

- If $m_{\tilde{\nu}} < m_{\chi^\pm}$, the chargino decays leptonically to $l\bar{\nu}$ (see Fig. 7) in $\sim 100\%$ of the cases, at least if the two-body decay to an on-shell W is kinematically suppressed. The three lepton flavours are produced in equal amounts if the chargino is mostly gaugino-like, while the $\tau\bar{\nu}$ final state dominates if the chargino is mostly higgsino-like since in that case it couples preferentially to the heaviest lepton. Here, it is assumed that the three scalar neutrino flavours are essentially mass degenerate.

The final state topologies expected to arise from the pair production of charginos are therefore:

- If $m_{\tilde{\nu}} > m_{\chi^\pm}$:
 1. An acoplanar pair of hadronic jets (or of hadronic jet systems) if both charginos decay to $\chi q\bar{q}'$. This occurs in 50% of the cases if W exchange dominates.
 2. An isolated lepton in a hadronic environment together with missing p_t if one of the charginos decays to $\chi q\bar{q}'$ and the other one to $\chi l\nu$. If W exchange dominates, this occurs in 40% of the cases (only 30% if the lepton is required to be an electron or a muon).
 3. An acoplanar lepton pair if both charginos decay to $\chi l\nu$. This however contributes only 10% of the final states if W exchange dominates, and this topology is therefore of little use in that case.
- An acoplanar lepton pair if $m_{\tilde{\nu}} < m_{\chi^\pm}$ since both charginos then decay to $l\bar{\nu}$. All combinations of the three lepton flavours contribute democratically if the gaugino component in the chargino is substantial. On the other hand, if the chargino is higgsino-like, an acoplanar τ pair is the dominant final state topology.

3.3.2 The case of heavy scalar neutrinos

A representative example has been fully worked out, corresponding to the following set of parameters:

- $m_{\chi^\pm} = 200 \text{ GeV}/c^2$
- $m_\chi = 100 \text{ GeV}/c^2$
- $m_{\tilde{\nu}} = 1 \text{ TeV}/c^2$
- $\sigma(e^+e^- \rightarrow \chi^+\chi^-) = 500 \text{ fb}$

This production cross-section and these chargino and LSP masses are obtained in the MSSM for $M_2 = 200 \text{ GeV}/c^2$, $\mu = -325 \text{ GeV}/c^2$ and $\tan\beta = 4$. In that case, the gaugino component in χ^\pm is larger than 90%.

The charginos decay to on-shell W s via $\chi^\pm \rightarrow \chi W$, leading to final state topologies purely hadronic in 50% of the cases, mixed hadronic-leptonic in 40% of the cases, and purely leptonic in 10% of the cases. Because it contributes so little while the background conditions are not substantially better than for the others, this last topology has not been analysed further in the presently considered case of heavy scalar neutrinos.

To select the non-purely leptonic topologies arising from chargino pair production, the following criteria have been applied to a sample of simulated events:

1. At least 5 charged particle tracks should be detected.
2. The polar angle of the sphericity axis with respect to the beam axis should be larger than 45° .
3. The missing transverse momentum should exceed $35 \text{ GeV}/c$.
4. The acoplanarity angle should be smaller than 150° .

To calculate the acoplanarity angle, the event is projected onto the plane perpendicular to the beam axis, the circularity axis is determined therein, and the event is divided into two hemispheres with respect to a plane perpendicular to the circularity axis. The angle between the directions of the momentum sums calculated in the two hemispheres is called the acoplanarity angle.

These cuts were designed to eliminate the bulk of the main background due to the reaction $e^+e^- \rightarrow W^+W^-$. Cut 2 takes advantage of the strong forward-backward peaking of the W -pair production. Cut 3 removes most of the W pairs in which both W s decay hadronically since these events should not show any significant missing energy; this is shown in Fig. 8. Cut 4 removes a large fraction of the W pairs in which one of the W s decays hadronically and the other leptonically; although these events are expected to exhibit some missing energy due to the neutrino from the leptonic W decay, the charged lepton momentum should be directed close to the line of flight of that W , and such events thus tend to remain coplanar.

At this point, one is left with 120 fb of W pairs and with 150 fb of signal. The remaining W pairs are largely due to cases where one of the W s experiences a very asymmetric leptonic decay leading to a rather soft charged lepton. The event sample is thus divided into two subsamples called mixed hadronic-leptonic or purely hadronic, a given event entering one or the other subsample according to whether it does or does not contain an isolated lepton. Such an isolated lepton has to be an electron or a muon, its momentum must exceed $5 \text{ GeV}/c$, and there should be less than 1 GeV additional energy in a cone of half opening angle 60° around its direction.

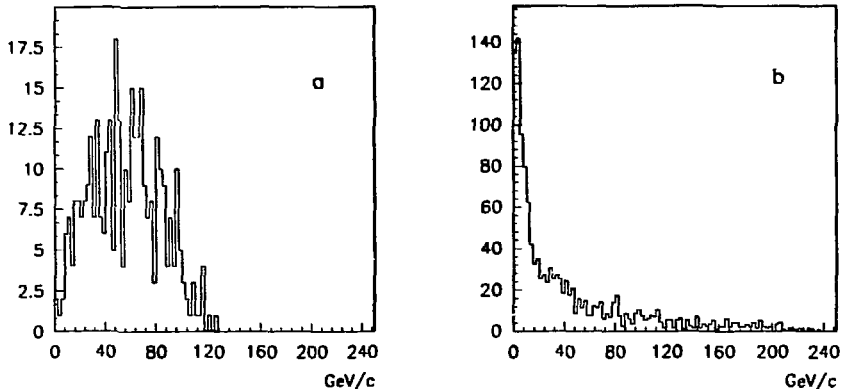


Figure 8: Missing transverse momentum for chargino pairs (a) and for W pairs (b) after cuts 1 and 2.

The purely hadronic subsample

In addition to not containing such a clearly isolated lepton, an event in the purely hadronic subsample should not contain a charged particle carrying more than 70% of the energy of the event hemisphere in which it lies. This removes W -decay leptons less isolated because of some leakage from the other W side, and also some of the $W \rightarrow \tau\nu$ decays. The W -pair background is thus reduced to 40 fb while 115 fb of the chargino signal are preserved.

However, the $W e \nu$ background has not been efficiently reduced up to now. It still contributes more than 700 fb, but it is readily removed by requiring a minimum value of 120 GeV/c^2 for the event total visible mass, as shown in Fig. 9. This is because, in such events, the electron tends to escape undetected in the beam pipe. The same cut also removes the $Z\nu\bar{\nu}$ background.

At this point, 74 fb of the chargino signal survive, while the W -pair background is reduced to 9 fb and the other backgrounds together to 11 fb. The W pairs can be further eliminated by requiring a minimum transverse missing mass of 200 GeV/c^2 , and the few events from $e^+e^- \rightarrow t\bar{t}$ by requiring a maximum visible mass of 220 GeV/c^2 . The signal finally selected has a cross-section of 63 fb, to be compared to a total background of (7.5 ± 2.5) fb.

If the same analysis is applied to the pair production of charginos of the same mass $m_{\chi^\pm} = 200 \text{ GeV}/c^2$, but with $m_\chi = 50 \text{ GeV}/c^2$, the accepted signal cross-section remains a comfortable 43 fb. On the other hand, it reduces to 5 fb if $m_\chi = 150 \text{ GeV}/c^2$. Although the analysis would probably be optimized

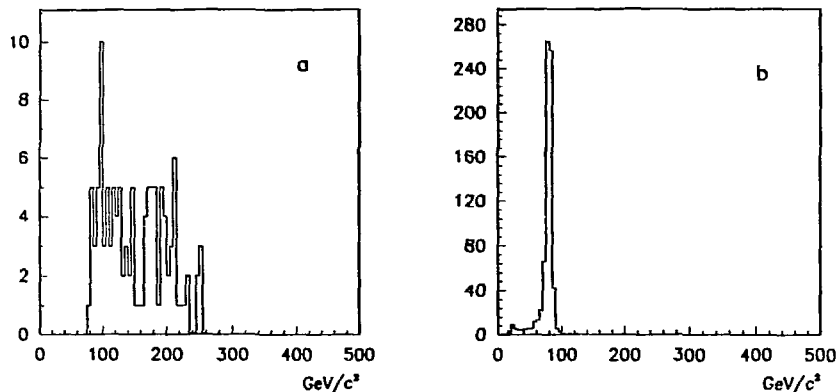


Figure 9: Visible mass for chargino pairs (a) and for $W e \nu$ events (b) in the purely hadronic subsample.

differently for such masses, there is no doubt that a smaller difference between the chargino and the LSP masses makes the detection harder, and certainly impossible at some point.

All these accepted signal cross-sections were obtained assuming a chargino production cross-section of 500 fb. However, it has been pointed out earlier that the latter may be reduced to 95 fb if $m_{\tilde{\nu}} \sim 250 \text{ GeV}/c^2$. This is still sufficient for a chargino-LSP mass difference of $100 \text{ GeV}/c^2$, but certainly no longer for a mass difference as low as $50 \text{ GeV}/c^2$.

The mixed hadronic-leptonic subsample

The principal background in this subsample comes from W -pairs in which one of the two W s decays leptonically. In such events, the three components of the momentum of the missing neutrino can be calculated from the knowledge of the initial state and from the measured total energy and momentum. Indeed, a fourth unknown quantity can even be allowed for in the calculation, a natural choice being the energy of a photon from initial state radiation or from beamstrahlung, assumed to be emitted along the beam direction and therefore undetected. The mass of the system formed by the isolated lepton and the reconstructed neutrino can then be calculated and, for events which really come from W -pair production, it should be compatible with the W mass. It can be seen in Fig. 10 that this is indeed the case most of the time. The method fails, however, for events in which the lepton comes from a τ decay, since there is more than a single neutrino missing in that case, or if photons were emitted by each of the e^+ and e^- incoming beams and lost in the beam pipe.

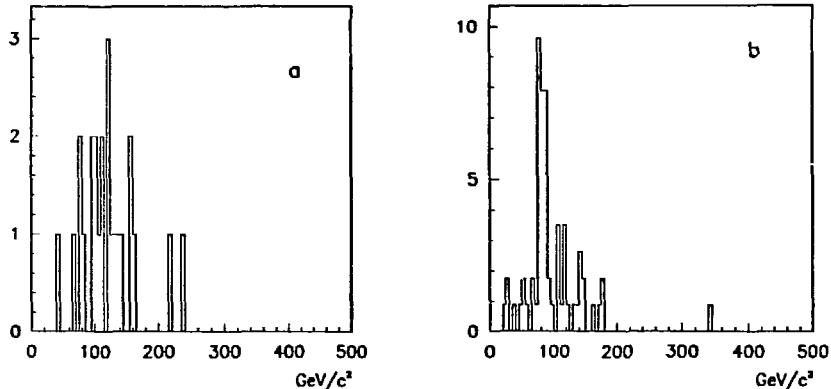


Figure 10: Reconstructed lepton-neutrino mass for chargino pairs (a) and for W pairs (b) in the mixed hadronic-leptonic subsample.

After a cut at $120 \text{ GeV}/c^2$ on the reconstructed lepton-neutrino mass, the total background is reduced to $(12.5 \pm 3.5) \text{ fb}$, of which 11.5 fb still come from W -pairs, but the accepted signal cross-section is only 12 fb . This method therefore adds little to the search in the purely hadronic subsample. On the other hand, it is less sensitive to the chargino-LSP mass difference: the accepted cross-section is still 8 fb if m_χ is taken equal either to $50 \text{ GeV}/c^2$ or to $150 \text{ GeV}/c^2$.

3.3.3 The case of light scalar neutrinos

The set of parameters used for the representative example worked out in the present case of light scalar neutrinos is the same as above except that:

- $m_{\tilde{\nu}} = 100 \text{ GeV}/c^2$ instead of $m_\chi = 100 \text{ GeV}/c^2$
- $\sigma(e^+e^- \rightarrow \chi^+\chi^-) = 100 \text{ fb}$

The minimum value of the production cross-section was chosen. This is over-conservative since this minimum is reached for a scalar neutrino mass larger than the one assumed here. For the chargino decay, it is first assumed that the gaugino component in χ^\pm is dominant, as is indeed the case for the set of MSSM parameters considered above. The three lepton flavours are then produced with equal probabilities in the $\chi^\pm \rightarrow l\tilde{\nu}$ decay process.

To select the acoplanar lepton pair topology arising from chargino pair production, the following criteria were applied to a sample of simulated events:

1. Exactly 2 charged particle tracks should be detected, and their transverse momenta should exceed 10 GeV/ c .
2. Both polar angles, measured with respect to the e^- beam direction, should satisfy the condition $-Q \cos \theta < 0.6$; here Q is the sign of the electric charge of the relevant particle.
3. No photon with an energy above 1 GeV is allowed to be detected except if its angle with one of the charged particles is smaller than 10° , or if the mass of any of the two photon-charged particle systems is smaller than 5 GeV/ c^2 .
4. The missing transverse momentum should exceed 35 GeV/ c .
5. The acoplanarity angle of the two charged particles should be smaller than 150° .
6. The event total visible mass should exceed 50 GeV/ c^2 ,
7. and it should not lie in the interval $(m_Z \pm 15 \text{ GeV}/c^2)$ if the charged particles are both electrons or both muons.

These cuts were primarily designed to eliminate the main background from W -pair production. In particular, Cut 2 takes advantage of the strong forward-backward charge asymmetry of the reaction $e^+e^- \rightarrow W^+W^-$, as shown in Fig. 11. Cut 3 removes $l^+l^-\gamma$ final states while preserving τ s from the signal which may decay to hadronic systems containing π^0 s. Cut 4 eliminates $l^+l^-\gamma$ events in which the photon remains in the beam pipe. Cuts 5 (see Fig. 12) and 6 eliminate most of the remaining W pairs while Cut 7 readily suppresses the ZZ and $Z\nu\bar{\nu}$ backgrounds.

The W -pair background is reduced to (8 ± 2.5) fb and the other backgrounds to (9 ± 3) fb while the accepted cross-section for the signal is 32 fb. The detection of such dominantly gaugino charginos should therefore not cause any particular problem.

If χ^\pm is a pure higgsino instead, the final state consists of acoplanar τ pairs exclusively for which the selection efficiency is about three times lower. However, the production cross-section is much larger since in that case there is no $\bar{\nu} t$ -channel exchange contribution and thus no destructive interference, which over-compensates the efficiency reduction.

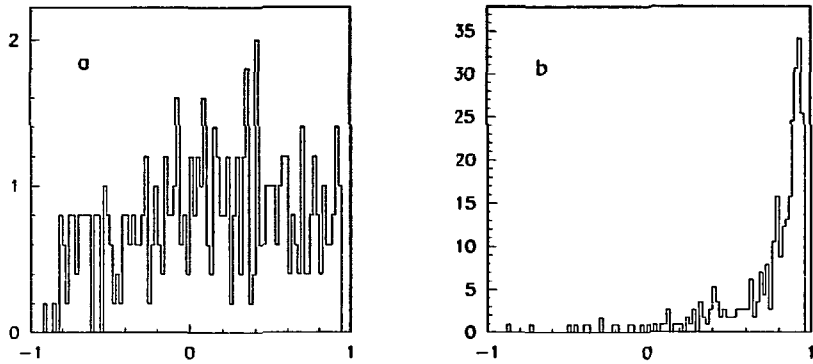


Figure 11: The larger $-Q \cos \theta$ for chargino pairs (a) and for W pairs (b) after cut 1.

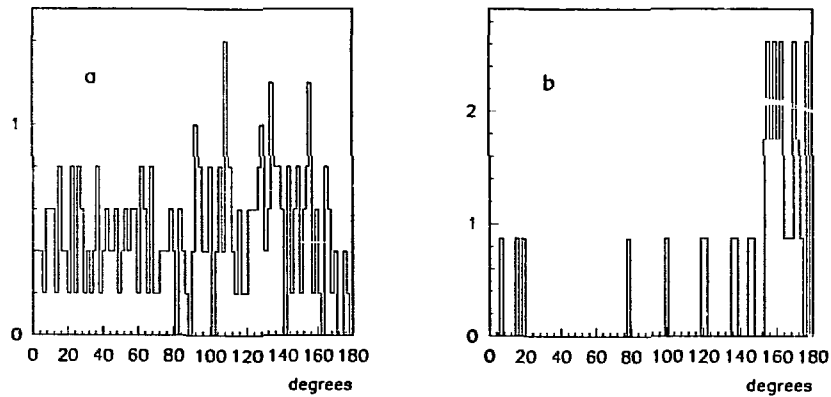


Figure 12: Acoplanarity angle for chargino pairs (a) and for W pairs (b) after cuts 1 to 4.

3.4 Implications of the chargino searches for the MSSM

The implications for the MSSM of the above discussed prospects for chargino discovery at a 500 GeV e^+e^- collider are summarized in Fig. 13.

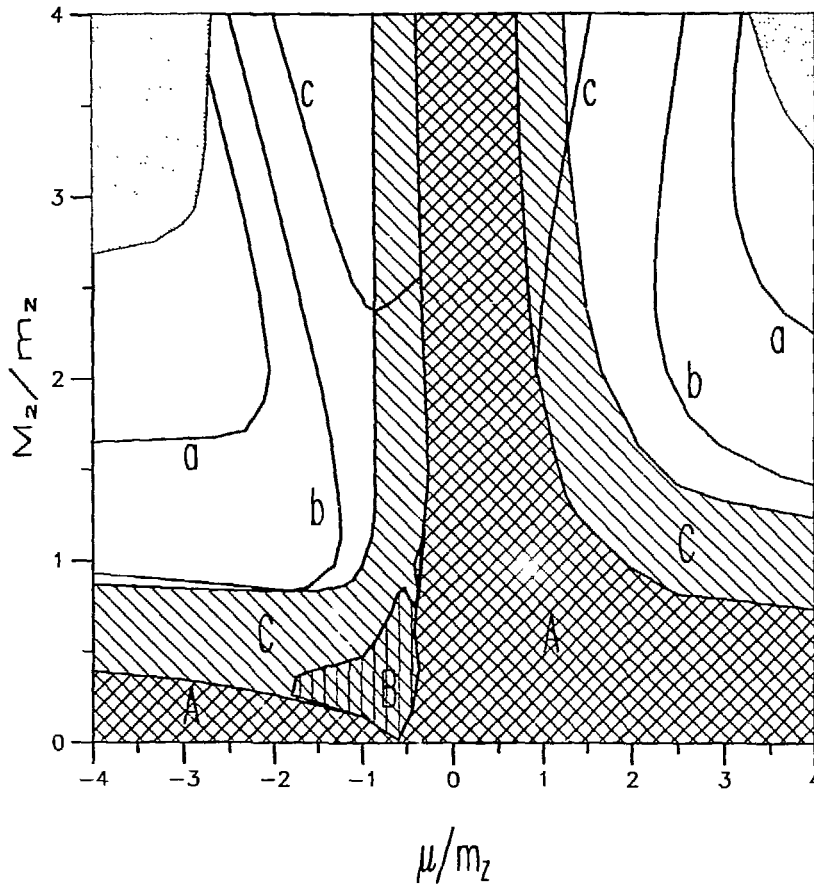


Figure 13: Impact of chargino searches on the MSSM.

The figure shows the $(M_2 \text{ vs. } \mu)$ plane; it has been drawn for $\tan \beta = 2$, but none of the conclusions is significantly affected by this choice. The cross-hatched region (A) is presently excluded by the full and invisible Z width measurements at LEP and the cross-hatched region (B) by the direct neutralino searches in Z decays[13]. The hatched region (C) is bounded by the curve $m_{\chi^\pm} = m_Z$ and corresponds roughly to the domain which should be explorable at LEP-200.

The grey regions extend beyond the curve $m_{\chi^\pm} = 250 \text{ GeV}/c^2$, thus indicating the domain not kinematically accessible in chargino pair production at a 500 GeV e^+e^- collider. The figure thus demonstrates how substantially larger the domain of parameter space of the MSSM potentially accessible at such a collider is, compared to the corresponding one at LEP-200.

It should however be kept in mind that the chargino searches will be increasingly less efficient as the mass difference $\Delta m = m_{\chi^\pm} - m_\chi$ becomes smaller. Curve (a) in Fig. 13 corresponds to $\Delta m = m_W$, Curve (b) to $\Delta m = 50 \text{ GeV}/c^2$ and Curve (c) to $\Delta m = 20 \text{ GeV}/c^2$. It is unlikely that mass differences smaller than this last value can be handled, and therefore that the regions above Curve (c) can be explored.

Unfortunately, neutralino searches will not help very much. Beyond the domain kinematically accessible for chargino pair production, the rates for neutralino production are exceedingly small. Besides, in the difficult region discussed above where Δm is small, the mass difference between χ and χ' is small too while the $\chi\chi'$ production cross-section is not larger than that of chargino pair production.

3.5 Search for scalar leptons

3.5.1 Scalar lepton production and signal topology

In all realistic supersymmetric models, the scalar lepton mass eigenstates are practically identical to the supersymmetric partners \tilde{l}_L and \tilde{l}_R of the left and right handed helicity states of the ordinary leptons. In the MSSM, the scalar lepton masses originate essentially from the universal scalar mass m_0 and from radiative corrections involving the gaugino mass M . These radiative corrections are substantially larger for \tilde{l}_L than for \tilde{l}_R ; for instance, if $m_{\tilde{l}_R} = 200 \text{ GeV}/c^2$ and $M_2 = 200 \text{ GeV}/c^2$ (which corresponds to $m_\chi = 100 \text{ GeV}/c^2$ if $\mu = -400 \text{ GeV}/c^2$ and $\tan\beta = 4$), then $m_{\tilde{l}_L} = 250 \text{ GeV}/c^2$. Therefore, the subsequent analysis concentrates on the detection of \tilde{l}_R only, although \tilde{l}_L could also be produced in some cases. On the other hand, the scalar partners of the same helicity states of the electron, of the muon and of the tau are expected to be practically mass degenerate.

The principal mechanisms for scalar lepton production in e^+e^- collisions are s -channel annihilation into a virtual photon or Z -boson, and also neutralino t -channel exchange in the case of scalar electrons (see Fig. 14). The pair production cross-sections for scalar muons or scalar taus are therefore identical and the scalar lepton mass $m_{\tilde{l}_R}$ is the only unknown quantity needed to calculate them. The production cross-section for scalar electrons, on the other hand,

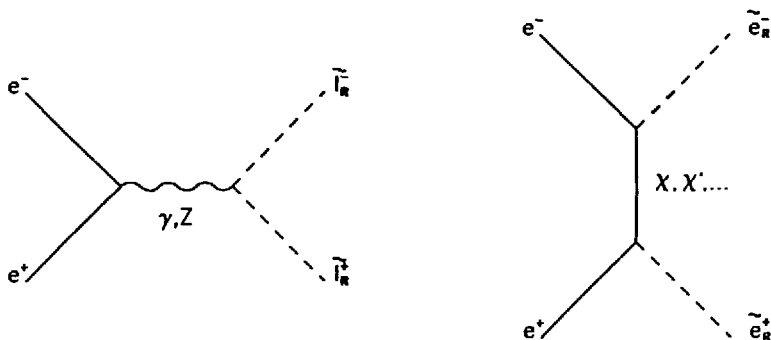


Figure 14: Diagrams involved in scalar lepton production.

depends on the masses and field contents of the various neutralinos. In the MSSM, it is therefore calculable, given $m_{\tilde{e}_R}$, once M_2 and, to a lesser extent, μ and $\tan\beta$ are given. The production cross-section is larger for scalar electrons than for the other scalar leptons; for instance, for $m_{\tilde{l}_R} = 200 \text{ GeV}/c^2$, the production cross-sections at 500 GeV are 23 fb for scalar muons or taus, and 120 fb for scalar electrons when $m_\chi = 100 \text{ GeV}/c^2$ (with $M_2 = 200 \text{ GeV}/c^2$, $\mu = -400 \text{ GeV}/c^2$, and $\tan\beta = 4$). These Born-level cross-sections are however reduced by as much as 60% because of initial state radiation and of beamstrahlung (with the rather severe spectrum assumed here).

The angular distribution for the production of scalar muons or taus is fully determined and is proportional to $\sin^2\theta$. On the other hand, because of the t -channel neutralino exchange, the angular distribution of scalar electrons shows some forward peaking, as can be seen in Fig. 15.

Scalar lepton pair production, followed by the decay $\tilde{l}_R \rightarrow l\chi$, has the characteristic signature of an acoplanar pair of leptons of the same flavour, with missing energy-momentum carried away by the χ s. Since scalar muons and scalar taus are expected to be practically mass degenerate and since their production mechanisms are identical, there is little to gain from a detailed investigation of both of these flavours, and since muons are easier to identify than taus, only scalar muon pair production is considered in the following. On the other hand, as stated above, scalar electron pair production occurs at a higher rate and with a different angular distribution, which justifies a specific investigation.

3.5.2 Analysis and results

Acoplanar charged particle pairs have already been analysed in the context of chargino pair production (see Section 3.3.3). The same selection criteria can therefore be applied, with the additional requirement that the two charged particles should be identified both as muons or both as electrons. These analyses have been reported by C. Van der Velde in the parallel session and are described in detail in Refs. [14] and [15]. The effect of some of the cuts is demonstrated in Figs. 15 and 16: as expected the transverse momentum efficiently discriminates the scalar lepton signal from the background from $\gamma\gamma$ -scattering, and the distribution of the lepton pair mass from the VV final state (with $V = Z$ or γ) exhibits a distinct peak at the Z mass, which the signal distribution naturally does not; in spite of the forward peaking of the produced scalar electron angular distribution, the decay electrons are distributed almost isotropically for large scalar electron masses, thus distinguishing the signal from the background of W pairs.

After electron or muon identification, the background level is reduced to 3 fb for electron pairs and to 2 fb for muon pairs, while the accepted signal cross-sections are 12 fb for scalar electrons and 6.5 fb for scalar muons, when $m_{\tilde{l}_R} = 200 \text{ GeV}/c^2$ and $m_\chi = 100 \text{ GeV}/c^2$ (with $\mu = -400 \text{ GeV}/c^2$ and $\tan\beta = 4$). The detection of such scalar leptons should therefore be easy at a 500 GeV e^+e^- collider.

The production cross-section is reduced for higher scalar lepton masses, and the search efficiency becomes lower as the mass difference between the scalar lepton and the LSP becomes smaller. Nevertheless, a signal to background ratio larger than two is obtained for scalar muon pairs with $m_{\tilde{\mu}_R}$ as high as $230 \text{ GeV}/c^2$ for small LSP masses, or for $m_{\tilde{\mu}_R} = 200 \text{ GeV}/c^2$ as long as $m_\chi < 150 \text{ GeV}/c^2$ [15]. In addition, in the extreme situation of a large $m_{\tilde{l}_R}$ together with a small $m_{\tilde{l}_R} - m_\chi$, other characteristic features of the signal may be used, such as the restricted range of the lepton momentum spectrum, in order to increase the significance level of the signal [14].

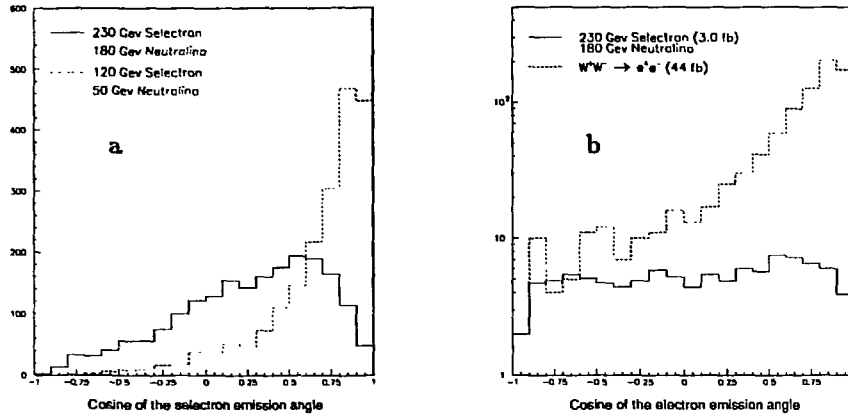


Figure 15: Angular distributions: a) of the produced scalar electrons for $m_{\tilde{e}_R} = 230 \text{ GeV}/c^2$ and $m_\chi = 180 \text{ GeV}/c^2$ (full histogram), and for $m_{\tilde{e}_R} = 120 \text{ GeV}/c^2$ and $m_\chi = 50 \text{ GeV}/c^2$ (dotted histogram); b) of the decay electrons for $m_{\tilde{e}_R} = 230 \text{ GeV}/c^2$ and $m_\chi = 180 \text{ GeV}/c^2$ (full histogram), and for the W -pair background (dotted histogram).

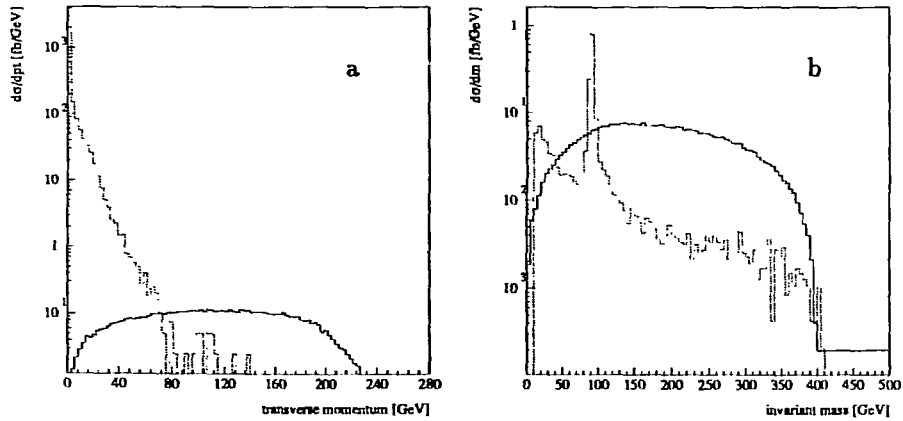


Figure 16: For a signal of scalar muons, with $m_{\tilde{\mu}_R} = 200 \text{ GeV}/c^2$ and $m_\chi = 100 \text{ GeV}/c^2$ (full histograms), distributions: a) of the transverse momentum, together with that from the $\gamma\gamma$ -scattering background; b) of the lepton pair mass, together with that from the VV background.

4 Conclusions

It has been shown that, with an integrated luminosity not larger than a few fb^{-1} collected at a 500 GeV e^+e^- collider, it will be possible to definitely rule out the MSSM if no neutral Higgs boson is detected. More positively, the simultaneous observation of the three neutral Higgs bosons of the MSSM can be expected in a large fraction of the parameter space of the model, which would decisively prove its validity.

It has also been shown that the potential of such a collider for the discovery of supersymmetric particles is indeed as large as anticipated. Even if the beamstrahlung conditions are as severe as in the example used for the present studies, and still with an integrated luminosity not larger than a few fb^{-1} , clear signals arising from the production of charginos or of scalar leptons can be observed almost up to the kinematic limit in spite of the large standard model backgrounds. Only if not enough visible energy is available in the decay of the produced supersymmetric particles can their discovery be made questionable. Whether such an unfortunate situation is likely or not to occur is left for the theorists to debate...

Acknowledgements

The following persons are gratefully acknowledged:

- A. Bartl and B. Mößlacher, for providing some supersymmetric process cross-section calculations,
- V. Bertin and G. Ganis, for helping with the chargino generator and with some calculations in the MSSM framework,
- R. Becker, R. Starosta and C. Van der Velde for making available their results on scalar leptons together with the relevant figures.

I am particularly indebted to Patrick Janot for his contribution to the analysis of the Higgs sector of the MSSM, for his numerous comments and suggestions, and for his critical reading of this manuscript.

References

- [1] F. Zwirner, these proceedings, and references therein.
- [2] P. Janot, "Testing the Neutral Higgs Sector of the MSSM with a 300-500 GeV e^+e^- Collider", preprint LAL 91-61, to be published in the proceedings of the Workshop "e⁺e⁻ Linear Colliders at 500 GeV: the Physics Potential", September 1991.
- [3] S. Komamiya, these proceedings.
- [4] P. Grosse-Wiesmann and D. Haidt, Contribution of the Higgs working group (P. Zerwas convener), to be published in the proceedings of the Workshop "e⁺e⁻ Linear Colliders at 500 GeV: the Physics Potential", September 1991.
- [5] ALEPH Coll., D. Decamp et al., Phys. Lett. 265B (1991) 475.
- [6] M. Contreras, "Search for the top quark and other new particles at $p\bar{p}$ colliders", proceedings of Physics in Collision 10, Duke Univ., June 1990, eds. A. Goshaw and L. Montanet.
- [7] M. Davier, "Searches for new particles at LEP", preprint LAL 91-48, to be published in the proceedings of the 1991 International Symposium on Lepton and Photon Interactions at High Energies, Genève, August 1991.
- [8] C. Dionisi et al., "Supersymmetric particles search at LEP-200", proceedings of the ECFA Workshop on LEP-200, Aachen, September 1986, eds. A. Böhm and W. Hoogland.
- [9] F. Pauss, "Beyond the Standard Model in pp Collisions", proceedings of the Large Hadron Collider Workshop, Aachen, October 1990, eds. G. Jarlskog and D. Rein.
- [10] C. Dionisi and M. Dittmar, "Prospects of supersymmetry searches in very high energy e^+e^- collisions", proceedings of the Workshop on Physics at Future Accelerators, La Thuile and Geneva, January 1987.
- [11] H.-U. Bengtsson and T. Sjöstrand, the PYTHIA version 5.5 Monte Carlo program, June 1991.
- [12] S. Ambrosanio and B. Mele, "Anomalous WWZ couplings at future e^+e^- colliders", Dipartimento di Fisica, Università di Roma "La Sapienza", preprint n.814, July 1991.

- [13] D. Decamp et al., "Searches for New Particles in Z Decays Using the ALEPH Detector", preprint CERN-PPE/91-149, September 1991, to be published in Physics Reports.
- [14] C. Van der Velde, "Experimental Aspects of Selectron Pair Searches", to be published in the proceedings of the Workshop " e^+e^- Linear Colliders at 500 GeV: the Physics Potential", September 1991.
- [15] R. Becker and R. Starosta, "Search for Scalar Muons at a Future 500 GeV e^+e^- Collider", to be published in the proceedings of the Workshop " e^+e^- Linear Colliders at 500 GeV: the Physics Potential", September 1991.